



Removal of acid blue 80 from aqueous solutions by adsorption on chemical modified bentonites

Fatima Gomri^a, Mokhtar Boutahala^a, Hassina Zaghouane-Boudiaf^a, Sophia A. Korili^b, Antonio Gil^{b,*}

^aLaboratoire de Génie des Procédés Chimiques (LGPC), Faculté de Technologie, Université Ferhat Abbas-Sétif1, Algeria

^bDepartment of Applied Chemistry, Building Los Acebos, Public University of Navarra, Campus of Arrosadia, Pamplona E-31006, Spain, email: andoni@unavarra.es (A. Gil)

Received 22 December 2015; Accepted 1 March 2016

ABSTRACT

Batch sorption experiments were performed to study the adsorption of Acid Blue 80 (AB80) dye from aqueous solutions using chemical modified bentonites as adsorbents. A raw-bentonite (RB) was converted to sodium bentonite (NaB). The NaB was activated by acid leaching with sulfuric acid in order to obtain a sample (ANaB) with modified adsorption properties. The NaB and ANaB samples were exchanged with two alkyltrimethylammonium bromides (alkyl = C16 and C18) to evaluate the effect of the carbon chain length on the AB80 adsorption. The obtained samples were characterized by XRD, fourier transform infrared spectroscopy, nitrogen adsorption at -196°C , and through the determination of pH_{zpc} . The effect of several operational parameters like pH, initial concentration of AB80, contact time, on the sorption behavior was studied. The adsorption kinetics were studied using pseudo-first-, pseudo-second-order and intraparticle diffusion models. The equilibrium adsorption data were analyzed using the Freundlich and Langmuir isotherm equation models. The Langmuir adsorption capacities (q_e) were found to be 201, 179, 170, and 126 mg/g at 30°C respectively for ANaBC18, NaBC18, ANaBC16, and NaBC16.

Keywords: Adsorption; Acid blue 80; Clay acid activation; Clay organo modification; Organoclay

1. Introduction

Dyes are important raw materials of some industries such as textile, leather, cosmetics, paper, printing, plastic, pharmaceuticals and food [1]. The wastewater discharged from these industries may contain a variety of organic compounds and toxic substances that exhibit toxic effects toward microbial populations and can be toxic and carcinogenic to animals [2].

Several technologies have been reported for dyes removal as coagulation, chemical oxidation, membrane separation, electrochemical process and adsorption [3]. Adsorption technique has been found to be an economical and effective treatment method for removal of dyes due to its sludge free clean operation [1]. There are many kinds of adsorbents for removing textile dyes from wastewater. Activated carbon is one of the most available adsorbents. However, the relatively high production and regeneration cost of activated carbon and approximately 10–25% loss

*Corresponding author.

during regeneration by chemical or thermal treatment makes this adsorbent economically less applicable [4].

Many low-cost adsorbents are being developed. Clay minerals are suitable for adsorption process due to their large specific surface area and nanometer scale size. Also, clays can be modified by the intercalation of organic cations into their interlayer surface. After the modification, the clays become organophilic and the negative charges of the clay surfaces are neutralized. Thus, organoclays are attractive for use as selective sorbents due to the organic layer [4]. Another chemical modification of clays is the treatment of materials with concentrated inorganic acids usually at high temperature. This process is known as acid activation. The most significant mechanism in the activation of natural bentonite is cation exchange by H^+ ions. These transformations in the bentonite give rise to significant changes in the cation exchange capacity (CEC), chemical and mineralogical characteristics of the bentonite. Acid treatments of the clay minerals retain the layered morphology and improve the adsorption properties of the clay by increasing the number of active sites [5,6].

The adsorption of basic dyes such as methylene blue, crystal violet and Rhodamine B (RB) onto cationic surfactant (hexadecyltrimethylammonium chloride) modified bentonite clay was investigated by Anirudhan et al. [7]. They found that organo modified clay shows better capacity for the removal of three dyes than the no-modified material. The adsorption process was found to be dependent on pH and initial dye concentration. In another study adsorption of reactive blue by organophilic nickel phyllosilicate was compared by Alencar et al. [8]. In their study contact time, pH, temperature and concentration were investigated and the set of data have shown favorable results for using the phyllosilicate as an adsorbent agent. Recently, Marçal et al. [9] were studied the capacity of a saponite modified with n-hexadecyltrimethylammonium bromide (CTBA) and/or 3-aminopropyltriethoxysilane (APTS) to adsorb and remove caffeine, as an example of emerging contaminant, from aqueous solutions. A maximum adsorption capacity at equilibrium of 80.54 mg/g was found by the authors.

In the present study, the surface of a commercial bentonite (RB) is purified and activated by NaCl and acid leaching with sulfuric acid and converted both into organo modified with two alkyltrimethylammonium bromides. The objective of the present work is to examine the effectiveness of organoclays for the removal of dyes such as Acid Blue 80 (AB80) from aqueous solutions. As others dyes, AB80 is a toxic substance but has a widespread use and high stability and it is very resistant to biological degradation so it is urgent to remove it from water.

2. Experimental

2.1. Materials

The bentonite clay was obtained from the Entreprise Nationale des substances Utiles et des Produits Non Ferreux, Hammam Bouhrara, Algeria. Its chemical composition was found to be as (mass %): 69.4 SiO_2 , 1.1 MgO , 14.7 Al_2O_3 , 0.8 K_2O , 0.3 CaO , 1.2 Fe_2O_3 , 0.5 Na_2O , 0.2 TiO_2 , 0.05 As, 11% loss of ignition. Its cation-exchange capacity (CEC) is 0.97 meq/g [6]. The surfactants hexadecyl and octadecyl-trimethylammonium bromide; sulfuric acid, AB80 (dye content 40%) were purchased from Sigma-Aldrich Chemicals. The structure of the dye is shown in Fig. 1.

2.2. Preparation of the adsorbents

The sodium bentonite (NaB) was prepared with a procedure similar to that of reported by Zaghoulane et al. [6]. 30 g of raw bentonite (RB) were mixed with 1 dm³ of 1 mol/dm³ NaCl solution and stirred for 24 h. After three successive treatments, the homoionic bentonite was dialyzed in deionized water until it was free of chloride. Then it was separated by centrifugation to eliminate all other solid phases (quartz, cristobalite, etc.). The NaB fraction (<2 μm) was recovered by decantation and dried at 80°C. The NaB was treated under mechanical stirring with 1 mol/dm³ H_2SO_4 solution at 90°C for 6 h. The mass ratio of NaB to the acid solution was 1:1. After activation, the solid was washed by distilled water until SO_4^{2-} free (test by $BaCl_2$) and dried at 80°C. The derivative is an acid-activated bentonite denoted by obtain a sample (ANaB).

The NaB and ANaB were treated with the cationic surfactant hexadecyl- and octadecyl-trimethylammonium bromide. The surfactant-modified bentonite was prepared by adding amounts of the cationic

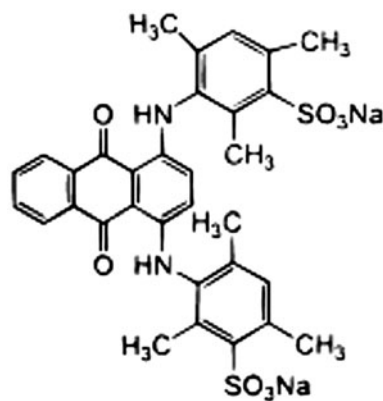


Fig. 1. Structure of AB80.

surfactant equivalent to 100% of the value CEC of the bentonite. The surfactant was dissolved in 1 dm³ of distilled water at 80°C and stirred for 3 h. A total of 10 g of sample (NaB and ANaB) were added separately to the 1 dm³ surfactant solution. The dispersions were stirred for 3 h at 80°C. The separated organo-bentonites were washed with distilled water. Washing was repeated until the supernatant solution was free of chloride ions, as indicated by the AgNO₃ test. The organo-bentonites were oven-dried at 80°C until the water was completely evaporated. The derivatives are NaBC16, NaBC18 (organo-bentonites) and ANaBC16, ANaBC18 (organo-acid activated bentonites).

2.3. Characterization techniques

The point of zero charge (pHpzc) was determined according to the method described by Benhouria et al. [10]. The initial pH values (pH_i) of 50 cm³ of aqueous solutions were adjusted to a pH range of 2–12 using 0.01 mol/dm³ of HCl or NaOH. Then, 0.05 g of adsorbent was added to each sample. The dispersions were stirred for 24 h at ambient temperature and the final pH of the solutions (pH_f) was noted. The difference between the initial pH (pH_i) and final pH (pH_f) values ($\Delta\text{pH} = \text{pH}_i - \text{pH}_f$) were plotted against pH_i, the point of intersection of the resulting curve with abscissa, at which $\Delta\text{pH} = 0$, gave the pHpzc. (Figure not showed).

X-ray diffractograms were obtained using a Bruker D8 advance diffractometer operating at 40 kV and 30 mA in the range 2 θ of 3°–70° and equipped with CuK α radiation source. Fourier transform infrared spectroscopy (FTIR) analysis of the adsorbent before and after modification were carried out in KBr pellets in the range of 400–4,000 cm^{−1}, with 4 cm^{−1} resolution using a SHIMADZU FTIR 8400 spectrometer. The structural characteristics of the materials were estimated from nitrogen adsorption results at −196°C using a static volumetric apparatus (Micromeritics ASAP 2010 adsorption analyzer). The samples were previously degassed at 200°C for 12 h before adsorption analysis under a vacuum of less than 0.1 Pa.

2.4. Dye adsorption experiments

The adsorption experiments were evaluated in batch mode. To measure the adsorption kinetics of AB80 onto the materials, 10 cm³ of aqueous dye solutions with an initial concentration of 50 mg/dm³ were placed in various glass tubes and mixed with 10 mg of the adsorbents without adjusting pH (pH around 6.6). After a shaking time was completed, the suspension was centrifuged at 2,500 rpm for 5 min. The effects of pH were studied in the range of 3–11 at

50 mg/dm³ of AB80 solutions, HCl and NaOH were used for the pH adjustments. The equilibrium concentration of dye solution was measured using a UV–vis spectrometer (ZUZI UV-4210) at a wavelength corresponding to the maximum absorbance (627 nm). The amount of the dye adsorbed by the adsorbents was calculated by the difference between the initial and remaining concentration of dye solution using the following equation:

$$q_{t,e} = V \cdot (C_0 - C_{t,e}) / m \quad (1)$$

where C_0 and C_t are the initial and liquid-phase concentrations at any time t of dye solution (mg/dm³), V (cm³) is the volume of the solution and m (mg) is the adsorbent mass.

Various AB80 solutions with several concentrations were prepared to determine the equilibrium adsorption capacity of the clay minerals. Typically, 10 mg of adsorbent was added to the glass tubes containing 10 cm³ of the dye solution with a concentration from 10 to 800 mg/dm³ for 4 h with a pH of 6.6. After shaking, the solution was separated from the solid by centrifugation. The remaining concentrations in the supernatants were determined by UV–visible spectrophotometer at a wavelength corresponding to the maximum absorbance (627 nm). The amount of dye adsorbed per unit mass of adsorbent at equilibrium was determined according to Eq. (1); where C_0 is the initial concentration of dye (mg/dm³), C_e is the concentration of dye (mg/dm³) at equilibrium, V (cm³) is the volume of the solution and m (mg) is the adsorbent mass.

3. Results and discussion

3.1. Characterization of the clays

The point of zero of charge (pHpzc) was the pH value of the solution surrounding the adsorbent when the sum of surface positive charges was equal to the sum of surface negative charges [11]. When solution pH < pHpzc, the adsorbents will react as a positive surface and as a negative surface when solution pH > pHpzc [6]. The pHpzc of samples NaB, NaBC16, NaBC18, ANaB, ANaBC16, and ANaBC18 has been determined as: 6.6, 6.8, 7.0, 5.8, 6.4, and 6.5.

The FTIR analysis was carried out to identify the functional groups present on the adsorbents (see Fig. 2) [12]. The absorption at 3,637 cm^{−1} was assigned to a stretching band of the inner OH unit within the clay structure, and the bands at 3,431 cm^{−1} are related to the OH vibrations of water molecules. The band at 1,632 cm^{−1} was assigned to the bending vibration of

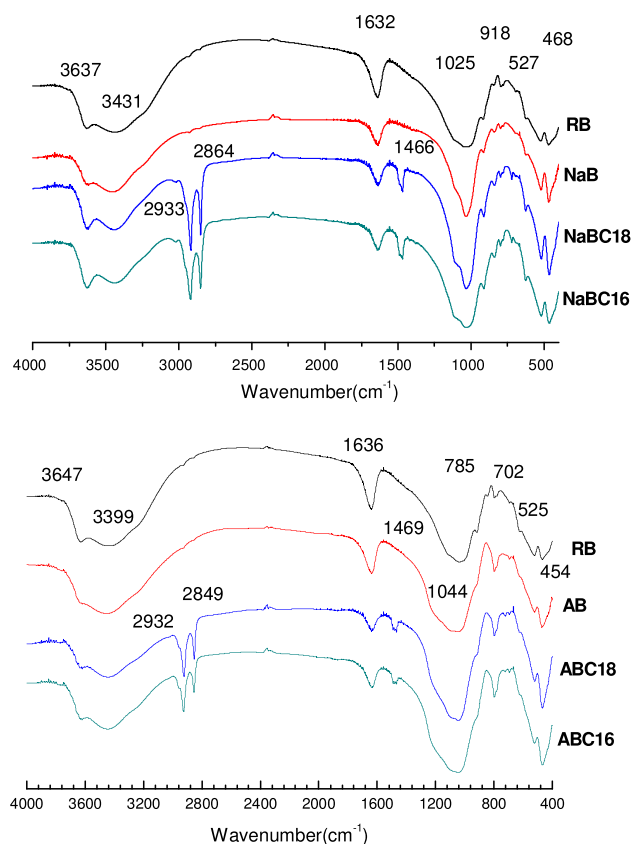


Fig. 2. FTIR spectra of the chemical modified clays.

water. Other characteristic vibrations of hydroxyl groups, the silicate anion and the octahedral cations are present in the IR spectrum of the adsorbents [13]. In all treated bentonites spectra, the intensities of these bands decreased substantially compared with those of RB [6]. A pair of strong bands at 2,864–2,933 cm^{-1} was observed in organo-bentonites. They can be assigned to the symmetric and asymmetric stretching vibrations of the methyl and methylene groups and their bending vibrations are between 1,632 and 1,466 cm^{-1} , supporting the intercalation of surfactant molecules between the silica layers [4]. FTIR spectroscopy is very sensitive to modification of the clay structure upon acid treatment. As protons penetrate into the clay layers and attack the OH groups, the resulting dehydroxylation connected with successive dissolution of the central atoms can be readily followed by changes in the characteristic absorption bands, attributed to vibrations of OH groups and/or octahedral cations. The bands at 3,399 and 1,636 cm^{-1} for water of hydration show a significant decrease in ANaB. The intensity of hydroxyl stretching bands at 3,647 cm^{-1} also reduces after the acid treatment. It is due to the removal of octahedral cations causing the loss of water and the

hydroxyl groups linked to them. This may be an acceptable evidence for the acid activation occurring on the bentonite. The SiO-stretching band (1,044 cm^{-1}) for ANaB occurs at the same position as that of RB, but its intensity decreases (see Fig. 2) [14].

The nitrogen adsorption-desorption results at -196°C for all the samples are shown in Fig. 3, from which it can be seen that these isotherms are of type II of the Brunauer, Deming, Deming and Teller classification [15]. The textural properties are summarized in Table 1. Acid-activation markedly affected nitrogen adsorption characteristics of the bentonite. After the activation, the nitrogen uptake relatively increased. After exchange with surfactant solutions, the nitrogen adsorption capacity of the organo-bentonites decreases and it was decreased more with the increase of alkyl chain length. In this case, the organic cations may

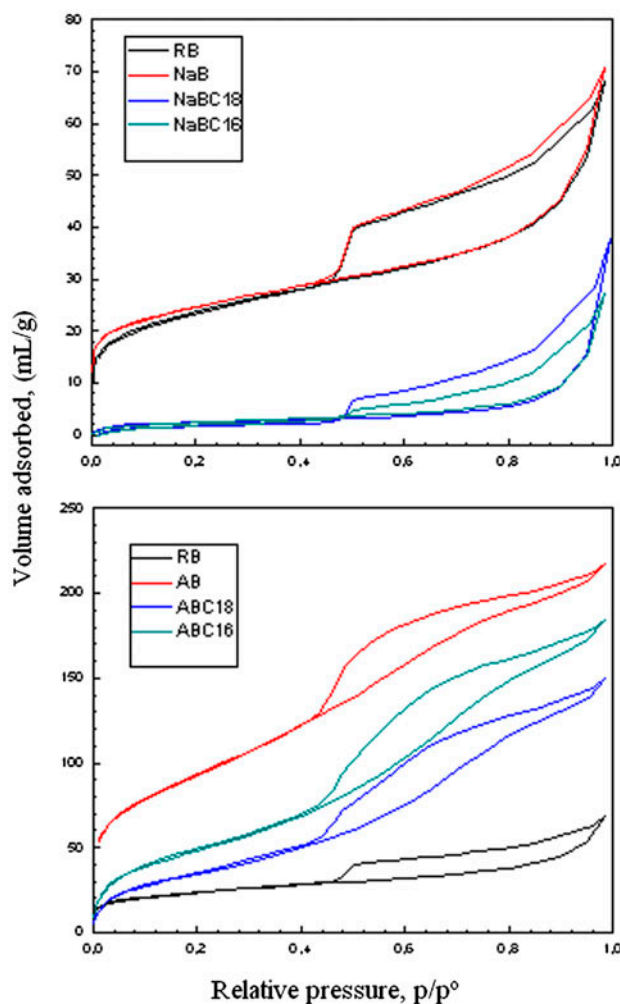


Fig. 3. N_2 adsorption-desorption isotherms of the chemical modified clays.

Table 1

Textural characteristics of the chemical modified clays

| Samples | S_{BET} (m^2/g) | S_{ext} (m^2/g) | V_{PT} (cm^3/g) | V_{HP} (cm^3/g) |
|---------|--|--|--|--|
| RB | 84 | 32 | 0.105 | 0.026 |
| NaB | 87 | 33 | 0.109 | 0.026 |
| NaBC16 | 9 | 8 | 0.042 | 0 |
| NaBC18 | 9 | 6 | 0.058 | 0 |
| ANaB | 337 | 42 | 0.335 | 0.254 |
| ANaBC16 | 180 | 55 | 0.286 | 0.180 |
| ANaBC18 | 130 | 49 | 0.232 | 0.136 |

block the access of nitrogen molecules to the adsorption sites and the pore network [6]. The results included in Table 1 shows also that, specific surface area and pore volume of ANaB decreased from $337 \text{ m}^2/\text{g}$ and $0.335 \text{ cm}^3/\text{g}$ to $180 \text{ m}^2/\text{g}$ and $0.285 \text{ cm}^3/\text{g}$ for ANaBC16 and $130 \text{ m}^2/\text{g}$ and $0.232 \text{ cm}^3/\text{g}$ for ANaBC18, indicating that surfactants with large molecular size occupied part of the inter-layer space resulting in inaccessibility of the internal surface to nitrogen molecules and the blocking of the pores in the organobentonites [6]. The micropore volume compared with a mesopore volume (see Table 1) of the samples indicates that bentonites have high mesoporosity.

XRD analysis can be used as useful tool to characterize the layer structure of bentonite before and after modification. The powder XRD patterns of organobentonites and organo-acid activated bentonites are shown in Fig. 4. It can be seen the reflection peak for NaB at $2\theta = 6.99^\circ$ with a $d(001)$ -spacing value of 12.63 \AA . After acid treatment, ANaB showed that the intensity of most of the XRD peaks decreased sharply ($d(001) = 15.91 \text{ \AA}$). Obviously, the dissolution of the smectite phase resulted in a successive dissolution of the octahedral sheet and the release of Al, Fe and Mg (Table 2). In addition, Al was removed from the tetrahedral sheet, which changed the electron density in the crystal structure and this affected the reflection intensity. After modification of NaB and AB with cationic surfactants, the $d(001)$ peaks in NaB and ANaB shifts to 21.85 , 22.69 , 19.11 , and 20.11 \AA in NaBC16, NaBC18, ANaBC16, and ANaBC18. This indicated that the surfactants hexadecyl (C16) and octadecyl (C18) trimethylammoniumions were entered in the interlayer space of bentonite and acid-bentonite by ion exchange [6].

3.2. Dye adsorption results

The pH is the most important factor that influences the adsorption process, because it can affect at the

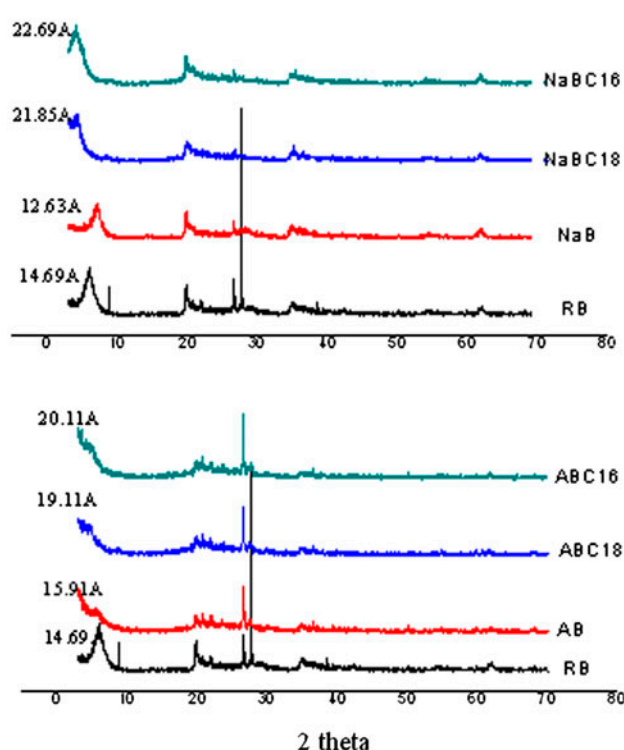


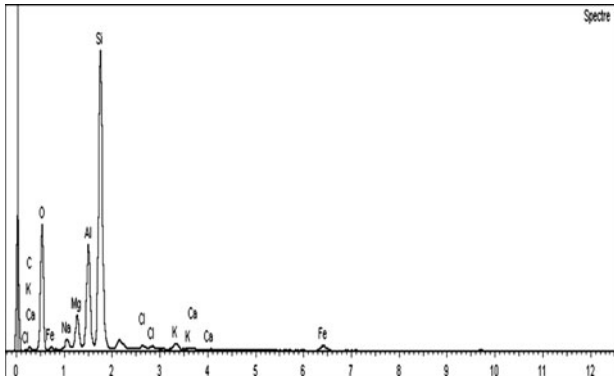
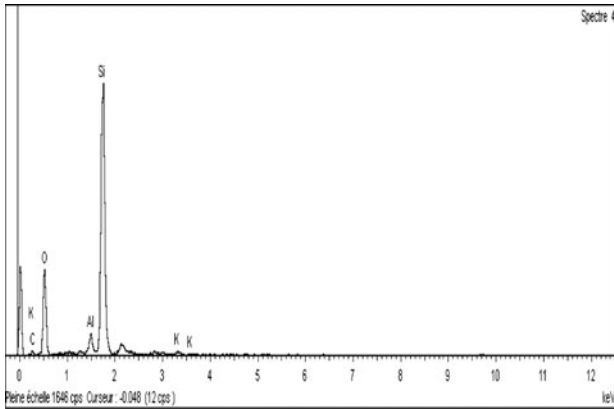
Fig. 4. X-ray diffractograms of the chemical modified clays.

same time the surface charge of the adsorbent, the ionization degree of functional groups of the adsorbate, and the mechanism of adsorption. The effect of pH observed in the adsorption of AB80 by organoclay is presented in Fig. 5. From the results included in this figure, the pH had no effect on the adsorption of AB80 onto the all organoclays.

The kinetics of the AB80 dye adsorption on the prepared adsorbents were determined in the same operating conditions. The plot of adsorption capacity vs. the contact time at was shown in Fig. 6. It was evident from the figures that the dye removal was rapid in the initial stages of contact time and reached equilibrium already after 40 min. The rapid adsorption at

Table 2

Chemical characterization of samples NaB (A) and ANaB (B) from Energy Dispersive X-ray Analysis (EDXA). The EDXA spectra of the samples are also included

| NaB | Mass (%) | |
|------|----------|---|
| C | 4.1 |  |
| O | 45.5 | |
| Na | 2.2 | |
| Mg | 2.6 | |
| Al | 10.1 | |
| Si | 31.6 | |
| K | 0.9 | |
| Fe | 2.3 | |
| ANaB | Mass (%) | |
| C | 10.3 |  |
| O | 51.4 | |
| Mg | 0.3 | |
| Al | 2.2 | |
| Si | 35.0 | |
| K | 0.6 | |
| Fe | 0.2 | |

the initial contact time can be attributed to the abundant availability of active sites on the adsorbent surfaces. Afterwards with the gradual occupancy of these sites, the adsorption became less efficient [16].

In order to investigate the adsorption process of AB80 on the adsorbents, pseudo-first-order, pseudo-second-order and the intra-particle diffusion model are used and applied to test the experimental data. The first-order rate equation, or the so-called Lagergren equation, can describe the initial phase in adsorption process and with the progressing of adsorption, the adsorption data may deviate the fitted curve [16]. The second-order rate equation agrees with chemisorption as the rate-control mechanism [17]. It has frequently been employed to analyse adsorption data obtained from various experiments with several types of adsorbates and adsorbents, as reviewed by Liu and Shen [18]. According to intraparticle diffusion model [7], several mechanisms are involved and the adsorption process can be characterized into three

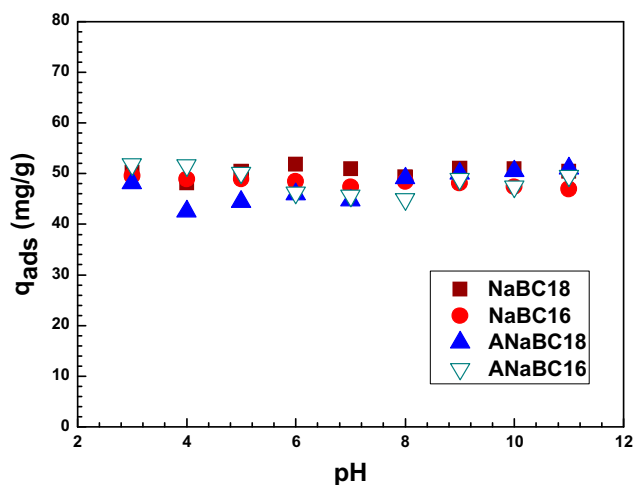


Fig. 5. Effect of the pH for the equilibrium adsorption data of AB80 on the chemical modified clays ($C_0 = 50 \text{ mg/dm}^3$, $T = 23^\circ\text{C}$, equilibrium time = 4 h).

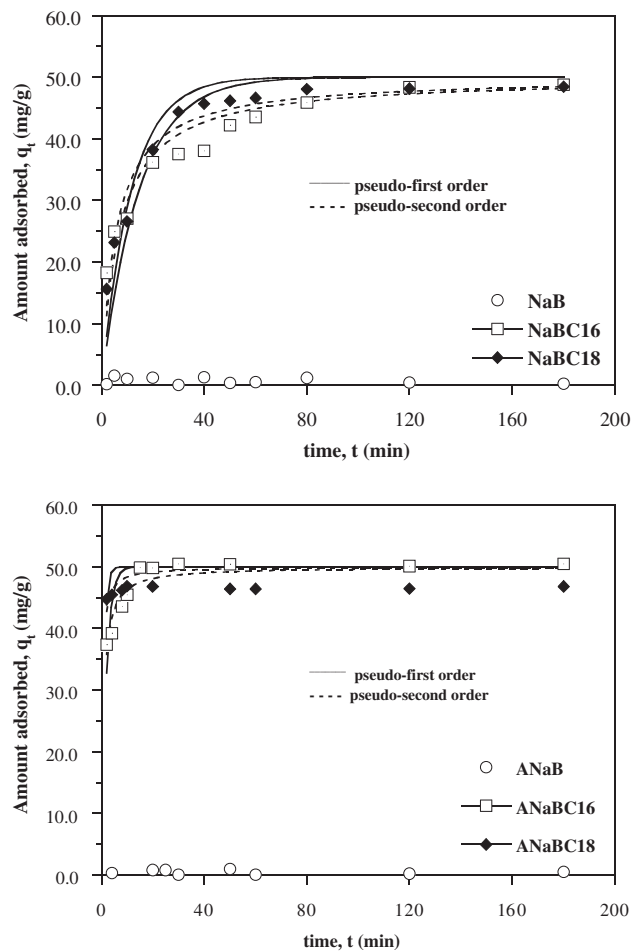


Fig. 6. Kinetic adsorption data for AB80 on the chemical modified clays ($C_0 = 50 \text{ mg/dm}^3$, $T = 23^\circ\text{C}$, pH 6.6).

Table 3
Pseudo-first- and -second-order parameters for AB80 adsorption by the chemical modified clays ($C_0 = 50 \text{ mg/dm}^3$, $T = 23^\circ\text{C}$, pH 6.6)

| | NaBC16 | NaBC18 | ANaBC16 | ANaBC18 |
|---------------------|--------|--------|---------|---------|
| <i>First-order</i> | | | | |
| k_1 (1/min) | 0.080 | 0.097 | 0.51 | 1.58 |
| χ^2 | 384 | 101 | 107 | 1.5 |
| R^2 | 0.78 | 0.96 | 0.73 | 0.78 |
| <i>Second-order</i> | | | | |
| k_2 (g/mg min) | 0.003 | 0.004 | 0.02 | 0.27 |
| χ^2 | 94 | 73 | 24 | 0.60 |
| R^2 | 0.95 | 0.97 | 0.95 | 0.92 |

steps: external surface adsorption, intraparticle diffusion which is the rate-limiting step and the final equilibrium which is very fast [14]. The results

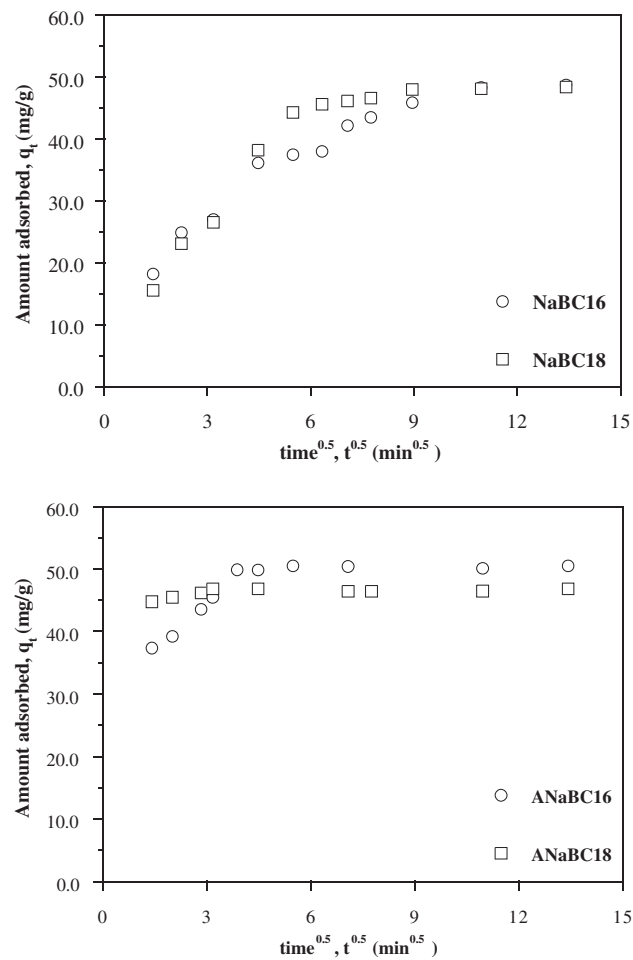


Fig. 7. Intraparticle diffusion model for the adsorption of AB80 on the chemical modified clays.

relating to kinetic behavior (see Table 3) reveal that the adsorption of AB80 can best be described as a pseudo-second-order linear reaction controlled by the interaction between the molecules of dye and the functional groups distributed on the surface of clay. The $q_{e,cal}$ (calculated q_e) values obtained from the pseudo-second-order showed excellent agreement with the $q_{e,exp}$ (experimental q_e).

The plots of the Morris-Weber relationship for the sorption of dyes, at initial concentration equal to 50 mg/dm^3 , by the organo-bentonite and organo-acid activated bentonites is shown in Fig. 7. Based on this figure, it may be seen that the intraparticle diffusion of dyes within the bentonite occurred in three stages [19]. The first linear portion included the adsorption period from 0 to 20 min, representing the external mass transfer or film diffusion (boundary layer) and the rapid distribution of dyes molecules onto the outer surface of bentonite. The second linear portion corresponds to the adsorption period of 20–90 min, which

represents the intra-particle diffusion and binding of dyes molecules into the internal active sites of the bentonite. Finally, the third linear portion (from 180 min) indicated a saturation of the adsorption process.

The most common representation of adsorbate concentration and quantity of material adsorbed is the adsorption isotherm. The equilibrium adsorption isotherm is fundamental for describing the interactive behavior between solutes and adsorbent, and is the basic requirement in the design of adsorption systems [20]. In this study, the Freundlich and Langmuir isotherm equations were used to model the experimental data.

The Freundlich isotherm model is an empirical equation employed to describe the adsorption processes in heterogeneous adsorbents, especially for organic compounds and highly interactive species on activated carbon [21]. The Freundlich isotherm equation can be expressed as follows:

$$q_e = k_F \cdot C_e^{1/m_F} \quad (2)$$

where q_e (mg/g) is the solid phase concentration of adsorbed species at equilibrium, C_e (mg/dm³) the equilibrium concentration of the adsorbate in the solution at equilibrium, and k_F and m_F are empirical constants that indicate adsorption magnitude and effectiveness.

Langmuir suggested a theory to describe the monolayer coverage of adsorbate on a homogeneous adsorbent surface. The adsorption isotherm is based on the assumption that sorption takes place at specific homogeneous sites within the adsorbent. Once an adsorbent molecule occupies a site, no further adsorption can take place at that site [21]. An equilibrium value can be reached and the saturated monolayer curve can be expressed as:

$$q_e = \frac{q_L \cdot k_L \cdot C_e}{1 + k_L \cdot C_e} \quad (3)$$

where q_e (mg/g) is the solid phase concentration of adsorbed species at equilibrium, C_e (mg/dm³) the equilibrium concentration of the adsorbate in the solution at equilibrium, and q_L (mg/g) and k_L (dm³/mg) are Langmuir constants representing the monolayer adsorption capacity and adsorption energy.

Adsorption isotherms for dye retention by all adsorbents are presented in Fig. 8. This isotherm indicates that dye have a high affinity for all adsorbents surface, particularly at low dye concentrations. Isotherm was characteristic of typical L-type adsorption

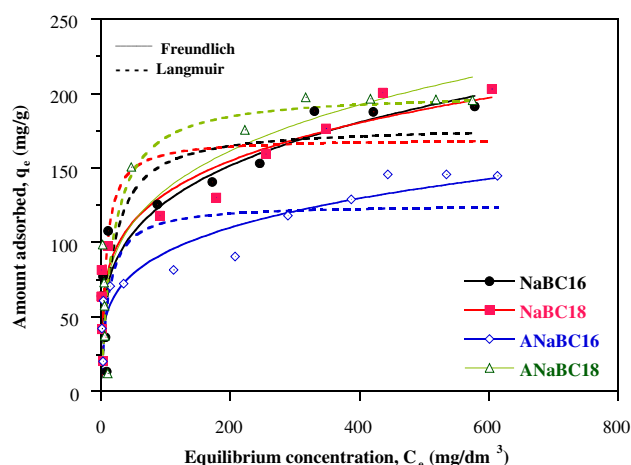


Fig. 8. Equilibrium adsorption data for AB80 on the chemical modified clays (equilibrium time = 4 h, $T = 23^\circ\text{C}$, pH 6.6).

Table 4

Freundlich and Langmuir parameters for AB80 adsorption by the chemical modified clays

| | NaBC18 | NaBC16 | ANaBC18 | ANaBC16 |
|-----------------------------|--------|--------|---------|---------|
| <i>Langmuir</i> | | | | |
| q_L (mg/g) | 179 | 170 | 126 | 201 |
| k_L (dm ³ /mg) | 0.061 | 0.147 | 0.093 | 0.055 |
| χ^2 | 11,553 | 13,039 | 5,922 | 10,465 |
| R^2 | 0.84 | 0.82 | 0.84 | 0.89 |
| <i>Freundlich</i> | | | | |
| k_F | 40 | 48 | 31 | 42 |
| m_F | 3.95 | 4.53 | 4.22 | 3.94 |
| χ^2 | 6,706 | 4,739 | 1,839 | 9,266 |
| R^2 | 0.91 | 0.94 | 0.95 | 0.91 |

reaction that represent a system where the adsorbate is strongly attracted by the adsorbent, generally by ion-ion exchange interactions that reach a saturation value represented by “the plateau” of the isotherm [22,23]. The analysis requires equilibrium to better understand the adsorption process. Non linear regression is used to determine the best-fitting isotherm, and the applicability of isotherm equations is compared by judging the correlation coefficients R^2 . The calculated constants of the two isotherm equations along with R^2 values are presented in Table 4. This table shows that the Freundlich isotherm gave the best correlation with R^2 value of 0.83 at 23°C . These coefficient obtained indicated that the adsorption isotherm of AB80 on organoclay can be applicable to Freundlich model. Freundlich model seems to be more coherent than other model. The applicability of this adsorption

Table 5

Comparison of monolayer adsorption of AB80 onto various adsorbents

| Adsorbents | Adsorption capacities (mg/g) | Refs. |
|------------------|------------------------------|-----------|
| ANaBC16 | 126 | This work |
| NaBC16 | 170 | This work |
| NaBC18 | 179 | This work |
| ANaBC18 | 201 | This work |
| Activated carbon | 171.0 | [24] |
| Mango seed | 9.2 | [25] |
| Guava seed | 1.1 | [26] |
| Activated carbon | 171.4 | [27,28] |

model to the investigated systems implies that heterogeneous surface conditions could occur simultaneously during the adsorption of AB80 on organoclay. k_F and m_F values are related to the adsorption capacity, and they can be used to distinguish adsorption performance. According to the present results, obtained k_F and m_F values indicated the higher adsorption capacity of organoclay [24] (see Table 4). Moreover, the Langmuir monolayer adsorption capacities were 126, 170, 179, and 201 mg/g for ANaBC16, NaBC16, NaBC18, and ANaBC18 which are compared with other adsorbents for AB80 adsorption described in Table 5. From the data summarized in this table, we can say also that hydrophobicity and organophilicity increased with increasing the alkyl chain, thus ANaBC18 becomes more hydrophobic and more organophilic than the other samples and enhanced the adsorption. In all samples, hydrophobic interactions of the dye should be involved with both alkylammonium ions and the remaining non-covered portion of siloxane surface [29].

4. Conclusions

In this work, textural and structural modifications of bentonite with alkyl ammonium molecules were studied. Organoclay was used to remove AB80 from aqueous phase. Hydrophobic nature of the adsorbent facilitates the adsorption process. The surface modification of organo-bentonite was examined by using various techniques; measurement of the d -spacing of the (0 0 1) peak indicates that increase in basal spacing was due to the introduction of organic cations into the bentonite interlayer. Simultaneously an important reduction of the specific surface area was obtained. Kinetics studies suggested that the adsorption mechanism of dye followed the pseudo-second model well. Experimental isotherms were analyzed by Langmuir and Freundlich models and their fitting results were

contrasted. From physical meaning interpretation of the model parameters, it was found that Freundlich model gave the best representation with two parameters described the experimental data well.

References

- [1] N. Gupta, A.K. Kushwaha, M.C. Chattopadhyaya, Adsorption studies of cationic dyes onto Ashoka (*Saraca asoca*) leaf powder, *J. Taiwan Inst. Chem. Eng.* 43 (2012) 604–613.
- [2] M.J. Ahmed, S.K. Dhedan, Equilibrium isotherms and kinetics modeling of methylene blue adsorption on agricultural wastes-based activated carbons, *Fluid Phase Equilib.* 317 (2012) 9–14.
- [3] F. Ahmad, W.M.A.W. Daud, M.A. Ahmad, R. Radzi, Cocoa (*Theobroma cacao*) shell-based activated carbon by CO₂ activation in removing of Cationic dye from aqueous solution: Kinetics and equilibrium studies, *Chem. Eng. Res. Des.* 90 (2012) 1480–1490.
- [4] S. Elemen, E.P.A. Kumbasar, S. Yapar, Modeling the adsorption of textile dye on organoclay using an artificial neural network, *Dyes Pigm.* 95 (2012) 102–111.
- [5] A. Gil, Y. El Mouzdahir, A. Elmchaouri, M.A. Vicente, S.A. Korili, Equilibrium and thermodynamic investigation of methylene blue adsorption on thermal- and acid-activated clay minerals, *Desalin. Water Treat.* 51 (2013) 2881–2888.
- [6] H. Zaghoulane-Boudiaf, M. Boutahala, S. Sahnoun, C. Tiar, F. Gomri, Adsorption characteristics, isotherm, kinetics, and diffusion of modified natural bentonite for removing the 2,4,5-trichlorophenol, *Appl. Clay Sci.* 90 (2014) 81–87.
- [7] T.S. Anirudhan, M. Ramachandran, Adsorptive removal of basic dyes from aqueous solutions by surfactant modified bentonite clay (organoclay): Kinetic and competitive adsorption isotherm, *Process Saf. Environ. Prot.* 95 (2015) 215–225.
- [8] J.M. Alencar, F.J.V.E. Oliveira, C. Airolidi, E.C. Silva Filho, Organophilic nickel phyllosilicate for reactive blue dye removal, *Chem. Eng. J.* 236 (2014) 332–340.
- [9] L. Marçal, E.H. de Faria, E.J. Nassar, R. Trujillano, N. Martín, M.A. Vicente, V. Rives, A. Gil, S.A. Korili, K.J. Ciuffi, Organically modified saponites: SAXS study of swelling and application in caffeine removal, *ACS Appl. Mater. Interfaces* 7(20) (2015) 10853–10862.
- [10] A. Benhouria, Md.A. Islam, H. Zaghoulane-Boudiaf, M. Boutahala, B.H. Hameed, Calcium alginate-bentonite-activated carbon composite beads as highly effective adsorbent for methylene blue, *Chem. Eng. J.* 270 (2015) 621–630.
- [11] L. Ding, B. Zou, W. Gao, Q. Liu, Z. Wang, Y. Guo, X. Wang, Y. Liu, Adsorption of Rhodamine-B from aqueous solution using treated rice husk-based activated carbon, *Colloids Surf. A* 446 (2014) 1–7.
- [12] M. Auta, B.H. Hameed, Modified mesoporous clay adsorbent for adsorption isotherm and kinetics of methylene blue, *Chem. Eng. J.* 198–199 (2012) 219–227.
- [13] M.M.F. Silva, M.M. Oliveira, M.C. Avelino, M.G. Fonseca, R.K.S. Almeida, E.C.S. Filho, Adsorption of an industrial anionic dye by modified-KSF-montmorillonite: Evaluation of the kinetic, thermodynamic and equilibrium data, *Chem. Eng. J.* 203 (2012) 259–268.

- [14] H. Zaghoulane-Boudiaf, M. Boutahala, Kinetic analysis of 2,4,5-trichlorophenol adsorption onto acid-activated montmorillonite from aqueous solution, *Int. J. Miner. Process.* 100 (2011) 72–78.
- [15] S. Brunauer, L.S. Deming, W.E. Deming, E. Teller, On a theory of the van der waals adsorption of gases, *J. Am. Chem. Soc.* 62(7) (1940) 1723–1732.
- [16] R. Liu, B. Zhang, D. Mei, H. Zhang, J. Liu, Adsorption of methyl violet from aqueous solution by halloysite nanotubes, *Desalination*. 268 (2011) 111–116.
- [17] G. Blanchard, M. Maunaye, G. Martin, Removal of heavy metals from waters by means of natural zeolites, *Water Res.* 18(12) (1984) 1501–1507.
- [18] Y. Liu, L. Shen, A general rate law equation for biosorption, *Biochem. Eng. J.* 38 (2008) 390–394.
- [19] K.K.H. Choy, J.F. Porter, G. Macky, Intraparticle diffusion in single and multicomponent acid dye adsorption from waste water onto carbon, *Chem. Eng. J.* 103 (2004) 133–145.
- [20] S. Azizian, M. Haerifar, H. Bashiri, Adsorption of methyl violet onto granular activated carbon: Equilibrium, kinetics and modeling, *Chem. Eng. J.* 146 (2009) 36–41.
- [21] A.W.M. Ip, J.P. Barford, G. McKay, Reactive black dye adsorption/desorption onto different adsorbents: Effect of salt, surface chemistry, pore size and surface area, *J. Colloid Interface Sci.* 337 (2009) 32–38.
- [22] Y. You, G.F. Vance, H. Zhao, Selenium adsorption on Mg–Al and Zn–Al layered double hydroxides, *Appl. Clay Sci.* 20 (2001) 13–25.
- [23] Y. You, H. Zhao, G.F. Vance, Surfactant-enhanced adsorption of organic compounds by layered double hydroxides, *Colloids Surf. A* 205 (2002) 161–172.
- [24] M.G.M. Ngumtchouin, M.B. Ngassoum, R. Kamga, S. Deabate, S. Lagerge, E. Gastaldi, P. Chaliier, M. Cretin, Characterization of inorganic and organic clay modified materials: An approach for adsorption of an insecticidal terpenic compound, *Appl. Clay Sci.* 104 (2015) 110–118.
- [25] M.M.D. Jiménez, M.P.E. González, V.H. Montoya, Performance of mango seed adsorbents in the adsorption of anthraquinone and azo acid dyes in single and binary aqueous solutions, *Bioresour. Technol.* 100 (2009) 6199–6206.
- [26] M.P.E. González, V.H. Montoya, Guava seed as an adsorbent and as a precursor of carbon for the adsorption of acid dyes, *Bioresour. Technol.* 100 (2009) 2111–2117.
- [27] M. Hadi, M.R. Samarghandi, G. McKay, Equilibrium two-parameter isotherms of acid dyes sorption by activated carbons: Study of residual errors, *Chem. Eng. J.* 160 (2010) 408–416.
- [28] G. McKay, A. Mesdaghinia, S. Nasser, M. Hadi, M.S. Aminabad, Optimum isotherms of dyes sorption by activated carbon: Fractional theoretical capacity & error analysis, *Chem. Eng. J.* 251 (2014) 236–247.
- [29] R.A. Schoonheydt, C.T. Johnston, Surface and interface chemistry of clay minerals, in: F. Bergaya, B.K.G. Theng, G. Lagaly (Eds.), *Handbook of Clay Science. I. Developments in Clay Science*, Elsevier, Amsterdam, 2006, pp. 87–113.